THE JOURNAL OF BIOLOGICAL CHEMISTRY VOL. 288, NO. 1, pp. 332–342, January 4, 2013

Differential Regulation of Extracellular Tissue Inhibitor of Metalloproteinases-3 Levels by Cell Membrane-bound and Shed Low Density Lipoprotein Receptor-related Protein 1

Received for publication, June 20, 2012, and in revised form, October 10, 2012 Published, JBC Papers in Press, November 19, 2012, DOI 10.1074/jbc.M112.393322

Simone D. Scilabra[‡§], Linda Troeberg[‡§1], Kazuhiro Yamamoto[§], Hervé Emonard[¶], Ida Thøgersen[‖], Jan J. Enghild[‖], Dudley K. Strickland[**], and Hideaki Nagase[‡§2]

*From the [‡]Department of Medicine, Imperial College London, London SW7 2AZ, United Kingdom, the [§]Kennedy Institute of Rheumatology, University of Oxford, London W6 8LH, United Kingdom, the [¶]University of Reims Champagne-Ardenne, FRE 3481 CNRS, 51100 Reims, France, the [‖]Department of Molecular Biology and Genetics, Aarhus University, 8000 Aarhus, Denmark, and the **Department of Surgery, University of Maryland, Baltimore, Maryland 21201*

Background: Tissue inhibitor of metalloproteinases-3 (TIMP-3) is endocytosed, but its regulatory mechanism is not well understood.
Results: TIMP-3 endocytosis occurs mainly through low density lipoprotein receptor-related protein-1 (LRP-1), but shed sLRP-1 binds TIMP-3.
Conclusion: TIMP-3-sLRP-1 complexes are retained extracellularly with metalloproteinase inhibitory activity.
Significance: LRP-1 is the master regulator of extracellular levels of TIMP-3.

Tissue inhibitor of metalloproteinases-3 (TIMP-3) plays a key role in regulating extracellular matrix turnover by inhibiting matrix metalloproteinases (MMPs), adamalysins (ADAMs), and adamalysins with thrombospondin motifs (ADAMTSs). We demonstrate that levels of this physiologically important inhibitor can be regulated post-translationally by endocytosis. TIMP-3 was endocytosed and degraded by a number of cell types including chondrocytes, fibroblasts, and monocytes, and we found that the endocytic receptor low density lipoprotein receptor-related protein-1 (LRP-1) plays a major role in TIMP-3 internalization. However, the cellular uptake of TIMP-3 significantly slowed down after 10 h due to shedding of LRP-1 from the cell surface and formation of soluble LRP-1 (sLRP-1)-TIMP-3 complexes. Addition of TIMP-3 to HTB94 human chondrosarcoma cells increased the release of sLRP-1 fragments of 500, 215, 160, and 110 kDa into the medium in a concentration-dependent manner, and all of these fragments were able to bind to TIMP-3. TIMP-3 bound to sLRP-1, which was resistant to endocytosis, retained its inhibitory activity against metalloproteinases. Extracellular levels of sLRP-1 can thus increase the half-life of TIMP-3 in the extracellular space, controlling the bioavailability of TIMP-3 to inhibit metalloproteinases.

The tissue inhibitors of metalloproteinases (TIMPs)[3] are a family of proteins that regulate the activity of metalloproteinases through formation of tight, noncovalent complexes in a 1:1 stoichiometry (1). Among the four mammalian TIMPs, TIMP-3 is unique in a number of respects. It has a broader inhibitory profile than the other TIMPs, being able to inhibit matrix metalloproteinases (MMPs) and the related metalloproteinases of the ADAM (a disintegrin and metalloproteinase) and the ADAMTS (a disintegrin and metalloproteinase with thrombospondin motifs) families (1). TIMP-3 is the only member of the family that can bind to the extracellular matrix (ECM) (2, 3), whereas the other TIMPs are readily extracted from the tissue. Studies using TIMP-3-null mice have indicated that it is the major regulator of metalloproteinase activities *in vivo*. Ablation of the *Timp3* gene leads to a number of defects in mice, including impaired lung development (4), dilated cardiomyopathy (5), increased apoptosis during mammary gland involution (6), and accelerated development of osteoarthritis upon aging (7). These are due to dysregulation of ECM turnover. In addition, uncontrolled activity of ADAMs, particularly ADAM17, resulted in elevated levels of TNFα and increased inflammation in murine models of liver regeneration (8), sepsis (9), and antigen-induced arthritis (7), and the phenotypes of the *Timp3*-null mouse are reflected in a number of human pathologies (for review, see Ref. 1). Thus, there is considerable interest in understanding factors regulating TIMP-3 levels, and it has been shown that transcription of TIMP-3 can be increased by the histone deacetylase SirT1 (10) and growth factors such as TGFβ (11) and oncostatin M (12) and reduced by promoter methylation (13). Translation of TIMP-3 can be reduced by

[1] Recipient of Arthritis Research United Kingdom Career Development Fellowship Grant 19466.
[2] Supported by National Institutes of Health Grant AR40994 through NIAMS and by a Arthritis Research United Kingdom Core Grant to the Kennedy Institute of Rheumatology. To whom correspondence should be addressed: Kennedy Institute of Rheumatology, University of Oxford, 65 Aspenlea Rd., London W6 8LH, United Kingdom. Tel.: 44-0-20-8383-4488; E-mail: hideaki.nagase@kennedy.ox.ac.uk.

[3] The abbreviations used are: TIMP, tissue inhibitor of metalloproteinase; ADAM, a disintegrin and metalloproteinase; ADAMTS, adamalysin with thrombospondin motifs; CS, chondroitin sulfate; CSPG, CS proteoglycan; ECM, extracellular matrix; FAM-AE∼LQGRPISIAK-TAMRA, carboxyfluorescein-Ala-Glu∼Leu-Asn-Gly-Arg-Pro-Ile-Ser-Ile-Ala-Lys-*N*,*N*,*N*′,*N*′-tetramethyl-6-carboxyrhodamine; HS, heparan sulfate; HSPG, HS proteoglycan; LRP-1, LDL receptor-related protein-1; miR, microRNA; MMP, matrix metalloproteinase; N-TIMP, N-terminal domain of TIMP; PPS, pentosan polysulfate; RAP, receptor-associated protein; sLRP-1, soluble LRP-1.

miR-21 (14), miR-221 and miR-222 (15), miR-181b (16), and miR-206 (17).

We have recently shown that TIMP-3 levels can be post-translationally regulated by endocytosis and intracellular degradation and suggested that this is an important factor determining extracellular levels of TIMP-3 (18). In the previous studies we used endocytic blockers to demonstrate the cellular uptake of TIMP-3. For example, HTB94 chondrosarcoma cells transfected with an expression plasmid for TIMP-3 produced high levels of *TIMP3* mRNA, but TIMP-3 protein was not detected in the conditioned medium. When heparin, pentosan polysulfate (PPS), or receptor-associated protein (RAP), an antagonist of ligand binding to low density lipoprotein (LDL) receptor and related receptors, was added to the cells, TIMP-3 accumulated in the medium. These studies suggested that the receptor responsible for TIMP-3 endocytosis is a member of the LDL receptor-related protein (LRP) family (18). There are 13 members in the mammalian LDL receptor family that endocytose a wide variety of ligands and deliver them to endosomes for degradation (19). Among them, LDL receptor-related protein 1 (LRP-1) endocytoses more than 30 ligands, including proteinase-inhibitor complexes and ECM proteins, making it an important regulator of ECM composition and turnover (20). LRP-1 comprises two chains, a 515-kDa α-chain that interacts with ligands via its four clusters of LDL receptor type A repeats and a noncovalently associated 85-kDa β-chain that tethers the receptor in the membrane and interacts with intracellular adaptors to direct endocytosis via clathrin-coated pits (20). LRP-1 can be shed from cell membranes, releasing a soluble form of the receptor, sLPR-1, that can act as a competitive inhibitor of ligand endocytosis (21, 22).

In this report, we used metabolically radiolabeled, isolated recombinant [^{35}S]TIMP-3 to investigate the endocytic pathways for TIMP-3 in more detail and analyzed the distribution of radioactivity in different cell fractions over time. Using LRP-1-deficient cells and sulfated proteoglycan mutant cells, we examined the contribution of LRP-1-dependent and LRP-1-independent pathways of TIMP-3 endocytosis. More importantly, our study has revealed that LRP-1 shed from the cell surface (sLRP-1) also binds to extracellular TIMP-3 and sequesters TIMP-3 in the medium and that TIMP-3 bound to sLRP-1 retained metalloproteinase inhibitory activity. This suggests that LRP-1 is a master regulator of extracellular levels of TIMP-3 and regulates ECM catabolism.

EXPERIMENTAL PROCEDURES

Materials—Heparin, de-*N*-sulfated heparin, chondroitin sulfate, hyaluronan, and Pronase were from Sigma-Aldrich. Dermatan sulfate from Calbiochem. PPS was from Arthropharm (Sydney, Australia), and GM6001 was from Elastin Products Co. (Owensville, MO). Dulbecco's modified Eagle's medium (DMEM), DMEM without L-glutamine or phenol red, L-glutamine, penicillin/streptomycin, fetal calf serum (FCS), hygromycin B, amphotericin B, and trypsin-EDTA were from PAA Laboratories (Somerset, UK). DMEM without L-glutamine, cysteine, methionine, or cystine was from MP Biomedicals (Solon, OH). The catalytic domain of human MMP-1 (24), recombinant His-tagged RAP (25), ADAMTS-4 lacking the C-terminal spacer domain (26), and nonradiolabeled FLAG-tagged TIMP-3 (27) were prepared as described previously.

Cell Culture—HTB94 human chondrosarcoma and THP-1 human monocytic acute leukemia cell lines were from American Culture Type Collection (Manassas, VA). Human uterine cervical fibroblasts were kindly provided by Akira Ito (Tokyo University of Pharmacy and Life Sciences, Japan). CHO-K1 and CHO-745 (28) were generously provided by Jeffrey D. Esko (Department of Cellular and Molecular Medicine, University of California San Diego, La Jolla, CA). MEF-1 and PEA-13 (homozygous LRP-1-deficient) (29) cells were generated as described previously. Syndecan-4-deficient and wild-type MEF (30) were kindly provided by John R. Couchman (Department of Biomedical Sciences and Biotech Research and Innovation Centre, University of Copenhagen, Copenhagen, Denmark). All cells were maintained in DMEM with 10% FCS, 100 units/ml penicillin, and 100 units/ml streptomycin at 37 °C in 5% CO_2.

Porcine articular cartilage chondrocytes were isolated from metacarpophalangeal joints within 24 h of slaughter (31). Cartilage was incubated with 1 mg/ml *Clostridium histolyticum* collagenase (Sigma-Aldrich) in 10 ml of DMEM with 10% FCS for 4 h at 37 °C. The digested material was passed through a cell strainer and washed, and cells were cultured in DMEM containing 10% FCS, 100 units/ml penicillin, 100 units/ml streptomycin, 2 mg/ml amphotericin B, and 10 mM HEPES at 37 °C in 5% CO_2.

Expression and Purification of [^{35}S]TIMP-3 and [^{35}S]N-TIMP-3—[^{35}S]TIMP-3 and ^{35}S-labeled N-terminal domain of TIMP-3 ([^{35}S]N-TIMP-3) were prepared by metabolic labeling. HEK-293/EBNA cells transfected with a pCEP4-based expression vector for C-terminally FLAG-tagged TIMP-3 (27) were grown to confluence in a 150-cm^2 flask, washed once, and starved for 2 h in serum-free DMEM without L-glutamine, cysteine, methionine, or cysteine. Cells were then grown for a further 4 days in serum-free DMEM without L-glutamine, cysteine, methionine, or cysteine, supplemented with 30 mM sodium chlorate and [^{35}S]Met/Cys (500 μCi of Redivue Pro-Mix L-[^{35}S] *in vitro* Cell Labeling Mix (GE Healthcare). Conditioned media were collected after 4 days, centrifuged to remove cell debris, and applied to a 2-ml anti-FLAG M2-agarose column (Sigma-Aldrich). The resin was washed extensively and bound protein eluted with 200 μg/ml FLAG peptide (Sigma-Aldrich). The purity of recombinant [^{35}S]TIMP-3 was confirmed by reducing SDS-PAGE and autoradiography. The active concentration of [^{35}S]TIMP-3 was determined by titration against a known concentration of the catalytic domain of MMP-1 (27).

Endocytosis of [^{35}S]TIMP-3—Cells were plated at a density of 1×10^6 cells/well and washed three times with serum-free DMEM. For some experiments, cells were then incubated for 1 h at 37 °C with GM6001 (10 μM), heparin, de-*N*-sulfated heparin, PPS, chondroitin sulfate, dermatan sulfate, hyaluronan (all at 200 μg/ml) or RAP (500 nM) in DMEM with 0.1% FCS before addition of [^{35}S]TIMP-3. As a control for agents diluted in dimethyl sulfoxide, the equivalent volume of dimethyl sulfoxide was added to separate wells. [^{35}S]TIMP-3 (1 nM) was added to cells in 2 ml of DMEM with 0.1% FCS. After a 0–24-h incubation, the conditioned medium was removed and 5% (v/v) tri-

chloroacetic acid (TCA) added (4 °C, overnight). The TCA-soluble fraction (2 ml) was separated from the TCA-insoluble fraction by centrifugation (13,000 rpm, 15 min, 4 °C). The TCA-insoluble pellet was dissolved in 1 N NaOH (500 μl). The cell layer was washed three times with ice-cold PBS and solubilized in 1 N NaOH (1 ml, 1 h, room temperature). Each fraction was mixed with 3 ml of scintillant (Goldstar Multipurpose Liquid Scintillation Mixture, Meridian, Surrey, UK) and radioactivity counted. TCA-soluble radioactivity present in the [^{35}S]TIMP-3 preparation prior to incubation with cells (5–15% of total radioactivity) was subtracted from the amount of TCA-soluble radioactivity at each time point. The amount of radioactivity in the different fractions was calculated as a percentage of the total amount of [^{35}S]TIMP-3 radioactivity added to the cells.

Endocytosis of Surface-bound [^{35}S]TIMP-3—[^{35}S]TIMP-3 (40 nM) in ice-cold TBS was added to cells and incubated for 2 h at 4 °C. To quantify cell surface binding of [^{35}S]TIMP-3, cells were washed twice in TBS, solubilized in 1 N NaOH (1 ml), and radioactivity quantified. In parallel experiments, endocytosis of cell surface-bound [^{35}S]TIMP-3 was quantified by washing cells in TBS and then incubating them for 2 h at 37 °C in prewarmed DMEM with 0.1% FCS. After 2 h, conditioned media were harvested and TCA-precipitated to quantify degraded [^{35}S]TIMP-3 (TCA-soluble counts in medium) and the amount of intact [^{35}S]TIMP-3 released from the cell surface (TCA-insoluble counts in medium). Cell layers were treated with 0.1% Pronase in serum-free DMEM on ice for 10 min, and then centrifuged (5000 rpm, 5 min, 4 °C) to allow quantification of cell surface-bound [^{35}S]TIMP-3 (Pronase-sensitive radioactivity) and intracellular [^{35}S]TIMP-3 (Pronase-resistant radioactivity, solubilized in 1 ml of 1 N NaOH).

Confocal Microscopy Analysis of TIMP-3 Endocytosis—HTB94, MEF-1, and PEA-13 cells were cultured on 18-mm glass coverslips coated with gelatin (0.1% w/v). Nonradiolabeled TIMP-3 (40 nM) was added to cells either alone or in combination with heparin (200 μg/ml) or RAP (500 nM) in phenol-red free DMEM with 0.1% FCS (2 h, 37 °C). Cells were then fixed with 3% paraformaldehyde in PBS (10 min, room temperature) and blocked with 5% (v/v) goat serum, 3% (w/v) bovine serum albumin in PBS (1 h, room temperature). Cells were permeabilized with PBS containing 0.1% (v/v) Triton X-100 (15 min, room temperature) and incubated with anti-FLAG M2 antibody (Sigma-Aldrich, F1804, 5 μg/ml, 1 h, room temperature). Alexa Fluor 488-conjugated goat anti-mouse IgG (Molecular Probes) was used to visualize the antigen signal (5 μg/ml, 1 h, room temperature). Actin was stained with Alexa Fluor 568-conjugated phalloidin (Molecular Probes). The signals were analyzed using a CCD camera-equipped microscope (Nikon TE-2000) with a 60× objective lens.

siRNA Targeting of Syndecan-1 Expression—HTB94 cells (1–1.5 × 10^5 cells) were transiently transfected with two 50 nM siRNAs targeting syndecan-1 (AM12432 and AM142557, Ambion) or scrambled (Ambion) using Lipofectamine 2000 for 3 h. After 24 and 48 h, expression of syndecan-1 was reduced by approximately 90% compared with the housekeeping gene *GAPDH*.

Isolation of sLRP-1 from Plasma—sLRP-1 was isolated from fresh-frozen human plasma by a modification of previously published methods (32). Plasma was diluted 5-fold with equilibration buffer (50 mM citrate, pH 6.0, 75 mM NaCl, 0.02% NaN_3) supplemented with proteinase inhibitor mixture (P8340, Sigma-Aldrich) and applied to a MacroPrep S ion exchange resin (Bio-Rad) equilibrated in the same buffer. The resin was washed extensively in equilibration buffer to remove unbound material, and bound proteins were then eluted in a gradient of 75–500 mM NaCl in equilibration buffer over 10 column volumes. Eluted fractions were analyzed by SDS-PAGE with silver staining and immunoblotting for LRP-1 using the 8G1 antibody (Abcam).

ELISA Detection of TIMP-3 Binding to sLRP-1—High binding microtiter plates (Corning, NY) were coated with 0.4 nmol of sLRP-1 in 50 mM citrate, pH 6.0, 75 mM NaCl overnight. Wells were blocked using 3% BSA-PBS (1 h, 37 °C) and washed in PBS containing 0.1% (v/v) Tween 20 (Sigma-Aldrich) after this and each subsequent step. Wells were then incubated with recombinant TIMP-3 in blocking solution (0.15–20 nM, 3 h, 37 °C). Bound TIMP-3 was detected by incubation of wells with murine M2 anti-FLAG antibody (3 h, 37 °C) and then with an anti-mouse secondary antibody coupled to horseradish peroxidase (1 h, 37 °C) (DAKO). Hydrolysis of tetramethylbenzidine substrate (KPL, Gaithersburg, MA) was measured at 450 nm using an EL-808 absorbance microplate reader (BioTek).

Inhibitory Activity of TIMP-3 Remnants—HTB94 cells were treated with or without TIMP-3 (1 nM) for 0, 24, or 48 h in serum-free, phenol red-free DMEM. Conditioned media were collected and centrifuged (13,000 rpm, 15 min, 4 °C) to remove cell debris. Recombinant ADAMTS-4 lacking the C-terminal spacer domain (1 nM) was incubated with dilutions of the media or with purified recombinant TIMP-3 in assay buffer (50 mM Tris-HCl, 150 mM NaCl, 10 mM $CaCl_2$, 0.05% Brij, 0.02% NaN_3) for 1 h at 37 °C. Residual activity against the fluorescent peptide substrate carboxyfluorescein-Ala-Glu∼Leu-Asn-Gly-Arg-Pro-Ile-Ser-Ile-Ala-Lys-*N*,*N*,*N*′,*N*′-tetramethyl-6-carboxyrhodamine (FAM-AE∼LQGRPISIAK-TAMRA, custom synthesized by Bachem, Switzerland) was determined (0.5 μM, excitation wavelength 485 nm, emission wavelength 538 nm with 495-nm cut-off) (27).

Co-immunoprecipitation of sLRP-1 with TIMP-3—HTB94 cells were incubated in serum-free DMEM for 24 h, and the conditioned media collected and centrifuged (13,000 rpm, 15 min, 4 °C) to remove cell debris. TIMP-3-FLAG (1 nM) was added to the conditioned medium (10 ml) and incubated overnight at room temperature with mixing. The solution was then applied to an anti-FLAG M2-agarose affinity resin (1 ml) equilibrated in TBS, and the resin was washed extensively with 10 volumes of TBS. Bound proteins were eluted sequentially with 50 mM Tris-HCl, pH 7.5, 10 mM $CaCl_2$, 0.2% NaN_3 containing 1 M NaCl (2 × 0.5 ml) and then with the same buffer containing 150 mM NaCl and 200 μg/ml FLAG peptide (2 × 0.5 ml). Eluted samples were analyzed by SDS-PAGE and immunoblotting using M2 anti-FLAG and 8G1 anti-LRP-1 antibodies. A band corresponding to the LRP-1 immunoreactive band was excised from the silver-stained gel, digested with trypsin, and analyzed by mass spectrometry.

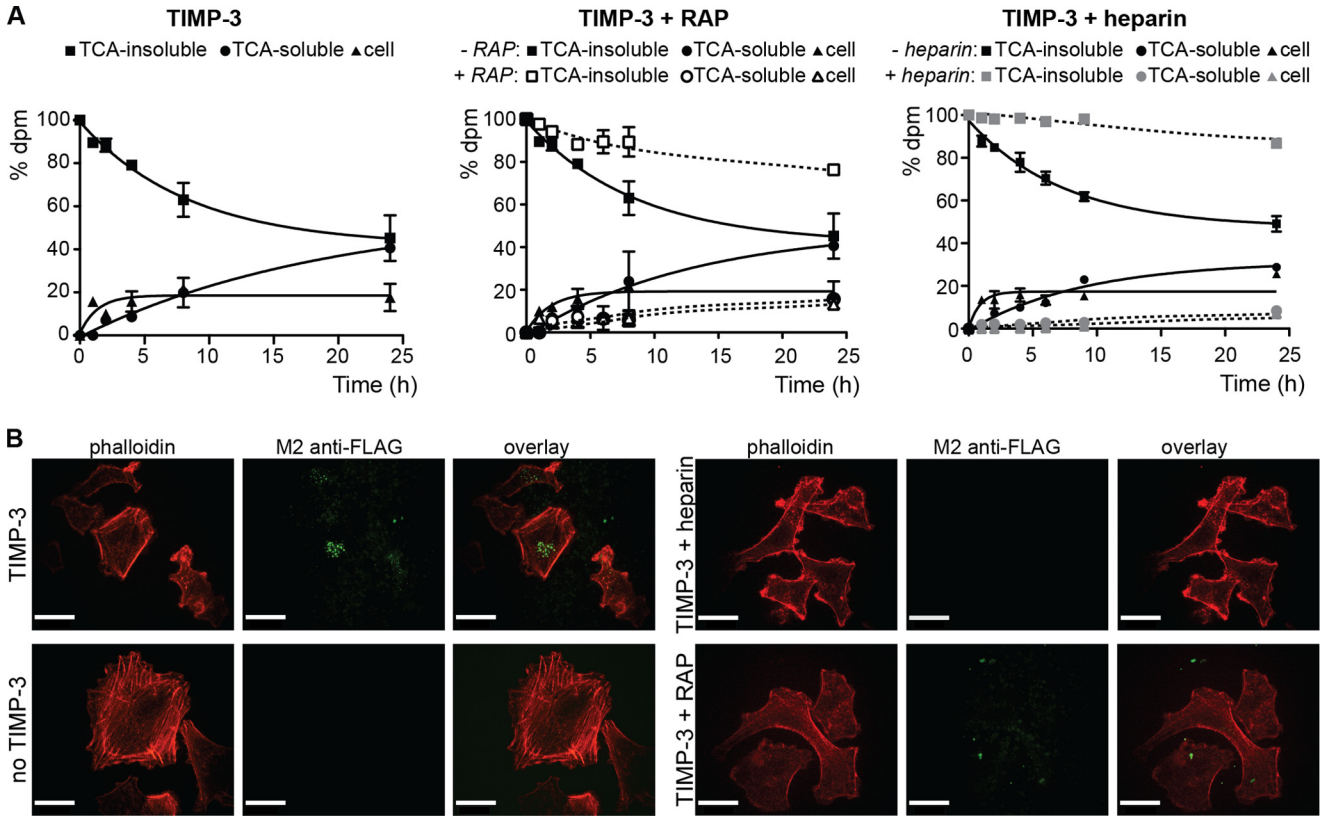

FIGURE 1. **TIMP-3 is endocytosed by HTB94 chondrosarcoma cells.** *A*, [^{35}S]TIMP-3 (1 nM) added to HTB94 chondrosarcoma cells in the absence or presence of RAP (500 nM) or heparin (200 μg/ml), and radioactivity in different cell fractions monitored over time ($n = 3$). TIMP-3, *black symbols*; TIMP-3 plus 500 nM RAP, *open symbols*; TIMP-3 plus heparin, *gray symbols*. *B*, confocal microscopy analysis of TIMP-3 endocytosis by HTB94 cells. Cells were incubated for 2 h at 37 °C with TIMP-3-FLAG (40 nM), either alone or with heparin (200 μg/ml) or RAP (500 nM). Control cells were incubated without TIMP-3-FLAG. Cells were washed and permeabilized, and endocytosed TIMP-3-FLAG was visualized using an M2 anti-FLAG antibody and an Alexa Fluor 488-labeled secondary antibody (*green* channel). The cytoskeleton was visualized using Alexa Fluor 568-labeled phalloidin (*red* channel). Images were gathered using a 60× objective lens. *Scale bars*, 41 μm.

RESULTS

TIMP-3 Is Endocytosed by HTB94 Cells—Metabolically labeled [^{35}S]TIMP-3 was purified and added to HTB94 cells in culture. The radioactivity in the TCA-insoluble fraction (intact [^{35}S]TIMP-3) of the conditioned medium decreased over 24 h, whereas that in the TCA-soluble fraction (degraded [^{35}S]TIMP-3 fragments) increased (Fig. 1*A*). Radioactivity was also detected in the cell and ECM layer (the cell-associated fraction). Treatment of the cell-associated layer with Pronase indicated that approximately half of the [^{35}S]TIMP-3 in this fraction was present within cells, with the remainder present on the cell surface and in the ECM. These results indicate that [^{35}S]TIMP-3 bound to the cell surface and was endocytosed and degraded by the cells, and peptide fragments were released back into the medium. [^{35}S]N-TIMP-3 was also endocytosed by HTB94 cells with indistinguishable kinetics, suggesting that the N-terminal domain contains the minimal structure required for endocytosis.

We reported previously that TIMP-3 accumulated in the conditioned medium of HTB94 cells in the presence of RAP, an antagonist of ligand binding to the LRP family of endocytic receptors (18). In line with this finding, RAP (500 nM) reduced endocytosis of [^{35}S]TIMP-3 by HTB94 cells, *i.e.* an increase in TCA-insoluble radioactivity and a decrease in TCA-soluble and cell-associated radioactivity (Fig. 1*A*). These data suggest that a member of the RAP-sensitive LRP family is involved in TIMP-3 endocytosis. Heparin (200 μg/ml) and PPS (200 μg/ml) similarly reduced endocytosis of [^{35}S]TIMP-3 (Fig. 1*A*), but de-*N*-sulfated heparin, dermatan sulfate, chondroitin sulfate, and hyaluronan (all at 200 μg/ml) had little effect. [^{35}S]TIMP-3 endocytosis was unaffected by addition of the broad spectrum metalloproteinase inhibitor GM6001, indicating that TIMP-3 is internalized without forming complexes with metalloproteinases. [^{35}S]TIMP-3 endocytosis and degradation were observed in a variety of other cell types, including porcine articular chondrocytes, human uterine cervical fibroblasts, and THP-1 human monocytic leukemia cells.

Cellular uptake of exogenously added TIMP-3 was also investigated by confocal microscopy. After incubation of HTB94 cells with recombinant TIMP-3-FLAG for 2 h at 37 °C, punctate staining for TIMP-3-FLAG was detected inside of the cells (Fig. 1*B*). This staining was absent in cells incubated without TIMP-3, indicating the specificity of the staining. The amount of intracellular fluorescent signal was greatly reduced by incubation of cells with RAP (500 nM) and completely abolished by incubation with heparin (200 μg/ml).

TIMP-3 Endocytosis Is Reduced in LRP-1-deficient Cells—Because TIMP-3 endocytosis was inhibited by RAP, we postulated that a member of the LRP family of receptors was involved in TIMP-3 endocytosis. We thus compared [^{35}S]TIMP-3 endocy-

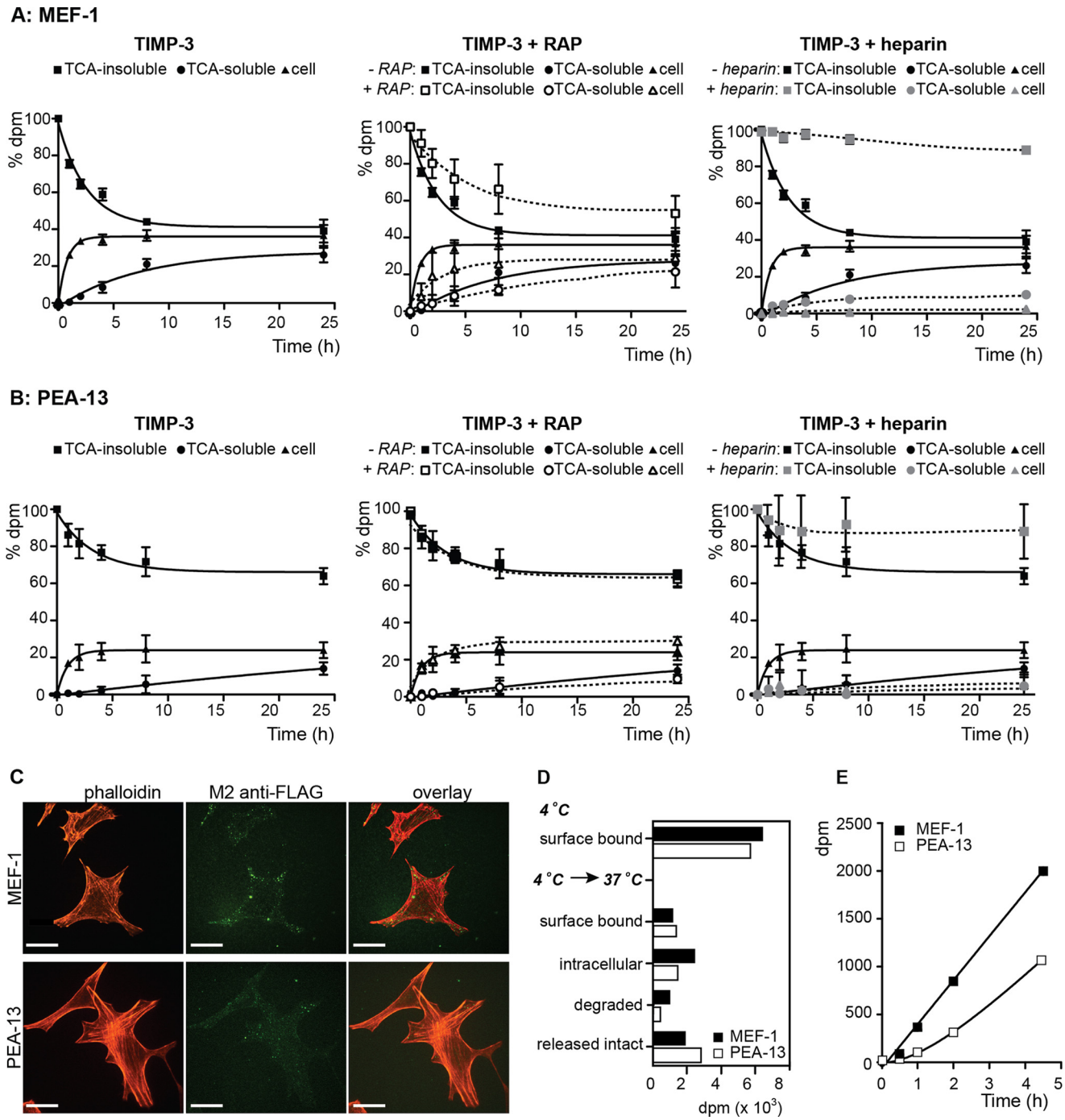

FIGURE 2. **LRP-1 contributes to [^{35}S]TIMP-3 endocytosis.** *A* and *B*, [^{35}S]TIMP-3 (1 nM) was added to MEF-1 (*A*) or PEA-13 (*B*) cells for 0–24 h, and radioactivity in the cell-associated fraction (*triangles*), as well as in the TCA-insoluble (*squares*) and TCA-soluble (*circles*) fractions of the conditioned media were quantified by scintillation counting ($n = 3$). TIMP-3, *black symbols*; TIMP-3 plus 500 nM RAP, *open symbols*; TIMP-3 plus 200 μg/ml heparin, *gray symbols*. *C*, confocal microscopy analysis of TIMP-3 endocytosis by MEF-1 and PEA-13 cells is shown. Cells were incubated for 2 h at 37 °C with TIMP-3-FLAG (40 nM), washed and permeabilized, and endocytosed TIMP-3-FLAG was visualized using an M2 anti-FLAG antibody and an Alexa Fluor 488-labeled secondary antibody (*green* channel). The cytoskeleton was visualized using Alexa Fluor 568-labeled phalloidin (*red* channel). Images were gathered using a 60× objective lens. *Scale bars*, 41 μm. *D*, [^{35}S]TIMP-3 (40 nM) was added to MEF-1 (*filled bars*) or PEA-13 (*open bars*) cells at 4 °C for 2 h to allow surface binding. Cells were warmed to 37 °C for 2 h, and surface-bound (Pronase-sensitive), intracellular (Pronase-resistant), degraded (TCA-soluble medium), and intact-released (TCA-insoluble medium) radioactivity was quantified. This result is representative of two separate experiments). *E*, TCA-soluble radioactivity was released by MEF-1 (*filled squares*) and PEA-13 (*open squares*) cells after surface binding of [^{35}S]TIMP-3. This result is representative of two separate experiments.

tosis by LRP-1-deficient mouse embryonic fibroblasts (PEA-13 cells) and wild-type cells (MEF-1). As shown in Fig. 2*A*, [^{35}S]TIMP-3 was readily endocytosed by MEF-1 cells with similar kinetics to that observed in HTB94 cells, but [^{35}S]TIMP-3 endocytosis was impaired in PEA-13 cells, with the rate of endocytosis approximately half of that observed in HTB94 and MEF-1 cells (Fig. 2*B*). This indicates that LRP-1 mediates a major pathway for TIMP-3 endocytosis but that an LRP-1-independent pathway also operates in these cells. Similar results were obtained using confocal microscopy, with endocytosed

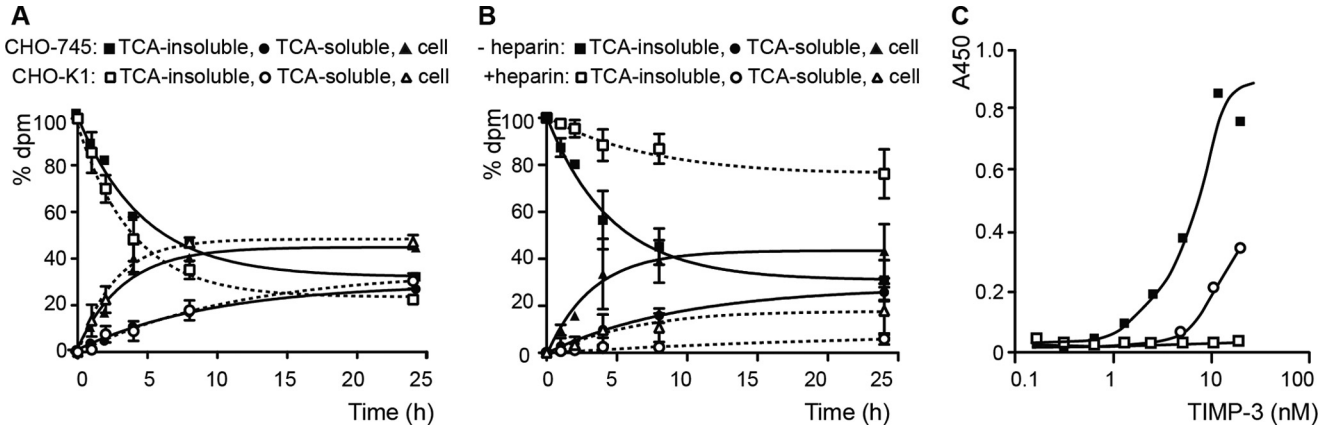

FIGURE 3. **Cell surface HSPGs and CSPGs are not required for TIMP-3 endocytosis.** *A* and *B*, [^{35}S]TIMP-3 (1 nM) was added to CHO-K1 (*solid lines* and *symbols*), CHO-745 (*A*, *dashed lines* and *open symbols*), or heparin-treated CHO-745 (*B*, *dashed lines* and *open symbols*) cells for 0–24 h, and radioactivity in the cell-associated fraction (*triangles*) as well as in the TCA-insoluble (*squares*) and TCA-soluble (*circles*) fractions of the conditioned media were quantified by scintillation counting ($n = 3$). *C*, Shed LRP purified from human plasma was coated onto microtiter plates, and binding of TIMP-3 (0.1–40 nM) in the absence (■) and presence (□) of 100 μg/ml heparin was measured using an M2 anti-FLAG antibody and a horseradish peroxidase-conjugate secondary antibody. Control wells (○) were not coated with sLRP.

TIMP-3-FLAG visible in vesicles within MEF-1 cells, but lower intracellular staining observed in PEA-13 cells (Fig. 2*C*). RAP inhibited [^{35}S]TIMP-3 endocytosis and degradation by MEF-1 cells to the level observed in PEA-13 cells (Fig. 2, *A* and *B*). In contrast, RAP had no effect on [^{35}S]TIMP-3 endocytosis by PEA-13 cells. Based on these observation we propose that LRP-1 is the only member within the LRP family that mediates [^{35}S]TIMP-3 endocytosis in these cells.

On the other hand, heparin strongly inhibited [^{35}S]TIMP-3 endocytosis by both MEF-1 and PEA-13 cells (Fig. 2, *A* and *B*). In this case, only a minimal decrease in TCA-insoluble radioactivity and little increase in TCA-soluble radioactivity in the medium were observed, and [^{35}S]TIMP-3 was barely detectable in the cell-associated layer.

We further investigated the role of LRP-1 in [^{35}S]TIMP-3 surface binding by adding 40 nM [^{35}S]TIMP-3 to cells at 4 °C. Comparable binding of [^{35}S]TIMP-3 to MEF-1 and PEA-13 cells was observed (Fig. 2*D*). Upon warming the cells to 37 °C, higher radioactivity was observed in MEF-1 cells, confirming their greater ability to endocytose [^{35}S]TIMP-3. Interestingly, both MEF-1 and PEA-13 cells released approximately one third of the surface-bound radioactivity back into the medium, indicating that there was a notable dissociation of [^{35}S]TIMP-3 from the cell surface under these experimental conditions. The release of TCA-soluble radioactivity by MEF-1 and PEA-13 cells was measured following cell surface binding of [^{35}S]TIMP-3 and warming of the cells to 37 °C. MEF-1 cells released approximately twice as much TCA-soluble radioactivity as PEA-13 cells Fig. 2*E*), confirming the existence of LRP-1-dependent and -independent endocytic pathways for TIMP-3.

Cell Surface Sulfated Glycosaminoglycans Are Not Involved in TIMP-3 Endocytosis—Because highly sulfated polysaccharides (*e.g.* heparin and PPS) blocked TIMP-3 endocytosis (18), we postulated that HSPGs or CSPGs may be involved in TIMP-3 endocytosis. To test this possibility we compared [^{35}S]TIMP-3 endocytosis by wild-type (CHO-K1) and mutant CHO-745 cells which lack HS and CS chains due to a mutation in xylosyltransferase (28). We observed no significant differences in the rate of [^{35}S]TIMP-3 endocytosis by CHO-K1 and CHO-745 cells (Fig. 3*A*), indicating that neither HSPG nor CSPG is required for the internalization of TIMP-3. [^{35}S]TIMP-3 endocytosis by both CHO-K1 and CHO-745 cells was partially inhibited by RAP (500 nM) (data not shown). Heparin (200 μg/ml) inhibited [^{35}S]TIMP-3 endocytosis by CHO-745 cells (Fig. 3*B*), indicating that the blocking effect of heparin is independent from the presence of HSPGs or CSPGS on the cell surface. Similarly, heparin blocked [^{35}S]TIMP-3 endocytosis by CHO-K1 cells. Interestingly, both CHO-745 and CHO-K1 exhibited a higher amount of cell-associated radioactivity than HTB94 or MEF cells. [^{35}S]TIMP-3 levels in this fraction were not affected by RAP, but were strongly inhibited by heparin.

We further investigated possible involvement of the syndecan family in TIMP-3 endocytosis because some protein ligands have been shown to bind to the core protein of these proteoglycans (33). Comparable endocytosis of [^{35}S]TIMP-3 was observed in syndecan-4-deficient and wild-type MEF, and siRNA targeting of syndecan-1 (leading to a 90% reduction in expression) had no effect on [^{35}S]TIMP-3 endocytosis.

Because heparin inhibits TIMP-3 endocytosis by cells lacking HSPG and CSPG, we tested whether heparin can directly interfere with the binding of TIMP-3 to LRP-1. We isolated sLRP-1 from human plasma and measured binding of TIMP-3 and TIMP-3-heparin complexes to immobilized sLRP-1 by ELISA. TIMP-3 bound readily to LRP-1, but upon preincubation with 100 μg/ml heparin, binding of TIMP-3 to LRP-1 was completely abolished Fig. 3*C*).

sLRP-1 Inhibits TIMP-3 Endocytosis—During the course of this study we noticed that for all of the cell lines we tested, TIMP-3 endocytosis was initially fast, but decreased over time, and little endocytosis was observed after 10 h. [^{35}S]TIMP-3 remaining in the medium at 24 h ([^{35}S]TIMP-3 remnants) appeared intact by reducing SDS-PAGE and autoradiography, with no fragmentation evident. The ability of TIMP-3 remnants to inhibit metalloproteinase activity was assessed by adding 1 nM TIMP-3 to HTB94 cells for 0, 24, or 48 h, after which time TIMP-3 remnants in the media were harvested and titrated

against 1 nM ADAMTS-4 *in vitro*. TIMP-3 collected after 0-h incubation on HTB94 cells completely inhibited 1 nM ADAMTS-4 (Fig. 4*A*). TIMP-3 harvested after 24- and 48-h incubation on HTB94 cells inhibited ADAMTS-4 activity by 60%, indicating that although the concentration of TIMP-3 in the medium had been reduced by endocytosis, the TIMP-3 remnants remaining in the medium retained their full inhibitory activity against metalloproteinases. These data indicate that TIMP-3 remnants had not undergone any substantial structural modification or inactivation.

We therefore considered whether the reduced rate of [^{35}S]TIMP-3 endocytosis was due to a change in the endocytic capacity of the cells. Although TIMP-3 has been shown to induce apoptosis in a variety of cell types (34), we found that incubation of HTB94 cells with 1 nM [^{35}S]TIMP-3 for 24 h had no effect on cell viability as measured by the 3-(4,5-dimethylthiazol-2-yl)-2,5-diphenyltetrazolium bromide (MTT) assay. Furthermore, pretreatment of HTB94 cells with nonradiolabeled TIMP-3 for 24 h did not alter the rate of endocytosis of subsequently added [^{35}S]TIMP-3.

We then investigated the possibility that TIMP-3 remnants in the medium were resistant to being taken up by the cells. To test this, [^{35}S]TIMP-3 remnants were added to naïve cells that had not previously been exposed to TIMP-3. Remnants collected from HTB94 cells after 24 h of incubation were largely resistant to endocytosis by naïve HTB94 cells, indicating that the [^{35}S]TIMP-3 remnants had become refractory to endocytosis (Fig. 4*B*). This phenomenon was further studied by incubating PEA-13 cells, which lack LRP-1, with [^{35}S]TIMP-3 for 24 h, and transferring the conditioned medium containing [^{35}S]TIMP-3 remnants to naïve MEF-1 cells. [^{35}S]TIMP-3 remnants from PEA-13 cells were readily endocytosed by naïve MEF-1 (Fig. 4*C*), whereas [^{35}S]TIMP-3 remnants from MEF-1 cells were resistant to endocytosis by naïve MEF-1 cells (Fig. 4*D*). Based on these results, we postulated that TIMP-3 became resistant to endocytosis as a result of association with sLRP-1 shed from cells into the conditioned medium during the culturing period.

sLRP-1 accumulated over time in the conditioned medium harvested from HTB94 cells grown in serum-free medium in the absence of TIMP-3 (Fig. 4*E*). Binding of TIMP-3 to sLRP-1 was investigated first by incubating TIMP-3-FLAG (1 nM) *in vitro* with the conditioned medium from HTB94 cells. After overnight incubation at ambient temperature, the mixture was applied to an M2 anti-FLAG resin, and bound proteins were eluted with FLAG peptide. Analysis of the eluted samples with the 8G1 anti-LRP-1 antibody indicated that LRP-1 was co-eluted with TIMP-3-FLAG by FLAG-peptide (Fig. 4*F*). The identity of the eluted LRP-1 band was further confirmed by mass spectrometry, confirming that TIMP-3 can interact with sLRP-1 shed into the conditioned medium of cells.

We also found that addition of TIMP-3 to HTB94 cells increases the release of sLRP-1 fragments of 500, 215, 160, and 110 kDa into the conditioned medium in a concentration-dependent manner, suggesting that the inhibitor can induce shedding and fragmentation of LRP-1 (Fig. 4*G*). When TIMP-3-FLAG (1 nM) was incubated with HTB94 cells for 24 h and conditioned medium was applied to an M2 anti-FLAG resin column, bound TIMP-3-FLAG co-eluted with the 500-kDa sLRP-1 and with LRP-1 fragments of 215, 160, and 110 kDa (Fig. 4*H*). This indicates that these fragments generated upon addition of TIMP-3 to the cells are capable of binding to the inhibitor.

DISCUSSION

Our study has revealed a new mechanism for regulating levels of TIMP-3 in the extracellular space. We previously reported that levels of this physiologically and pathologically important inhibitor can be post-translationally regulated by endocytosis (18). TIMP-3 accumulates in the medium of HTB94 chondrosarcoma cells and porcine articular chondrocytes treated with receptor-associated protein (RAP), an antagonist of ligand binding to the LRP family of endocytic receptors (18). Using radiolabeled TIMP-3 we investigated the kinetics of TIMP-3 endocytosis and degradation by LRP-1-deficient PEA-13 mouse embryonic fibroblasts and their wild-type counterpart. TIMP-3 endocytosis was substantially reduced in LRP-1-deficient PEA-13 cells compared with wild-type cells, indicating that LRP-1 is an important component of the TIMP-3 endocytic machinery. RAP, which inhibits ligand binding to all LRPs, had no effect on the residual endocytosis of TIMP-3 by PEA-13 cells, indicating that LRP-1 is the only member of the LRP family that mediates TIMP-3 endocytosis in mouse embryonic fibroblasts.

We compared the endocytosis of TIMP-3 by several cell types, including chondrosarcoma cells, porcine articular chondrocytes, fibroblasts, and monocyte-like THP-1 cells. All cell types showed similar kinetics for TIMP-3 endocytosis. The rate of TIMP-3 endocytosis was not constant over 24 h. After addition of [^{35}S]TIMP-3 to cells, endocytosis was initially rapid, but then slowed, so that only minimal endocytosis was observed after 10 h. We demonstrated that this reduction in endocytosis is due to interaction of TIMP-3 with a soluble form of LRP-1 shed from the cell surface into the medium. Different LRP-1 "sheddases" have been described, including ADAM10, ADAM12, ADAM17, MT1-MMP, and β-secretase (23, 35–38). Although the specific sites at which these enzymes cleave LRP-1 have not been characterized, shedding is known to involve cleavage of the β-chain of LRP-1, releasing a fragment of the β-chain in complex with the entire ligand binding α-chain from the cell membrane (39). Inflammation is a key stimulus for LRP-1 shedding. For example, interferon γ and LPS stimulate LRP-1 shedding by ADAM17 (35). Increased levels of sLRP-1 are detectable in the plasma of patients with rheumatoid arthritis, systemic lupus erythematous (35), and liver disease (32). sLRP-1 and lower molecular mass fragments of LRP-1 are found in brain and in cerebral spinal fluids and are increased in older people (23). Cholesterol depletion has also been found to stimulate LRP-1 shedding by MT1-MMP and ADAM12 (36). We observed LRP-1 shedding in the absence of any proinflammatory stimuli, and addition of IL-1 had no effect on the rate of TIMP-3 endocytosis by primary chondrocytes.[4] Because a number of the proposed LRP-1 sheddases are metalloproteinases, production of sLRP-1 should be inhibited by metalloproteinase inhibitors such as TIMP-3 and GM6001. However, we found that TIMP-3 could induce shedding of

[4] S. Scilabra and H. Nagase, unpublished observations.

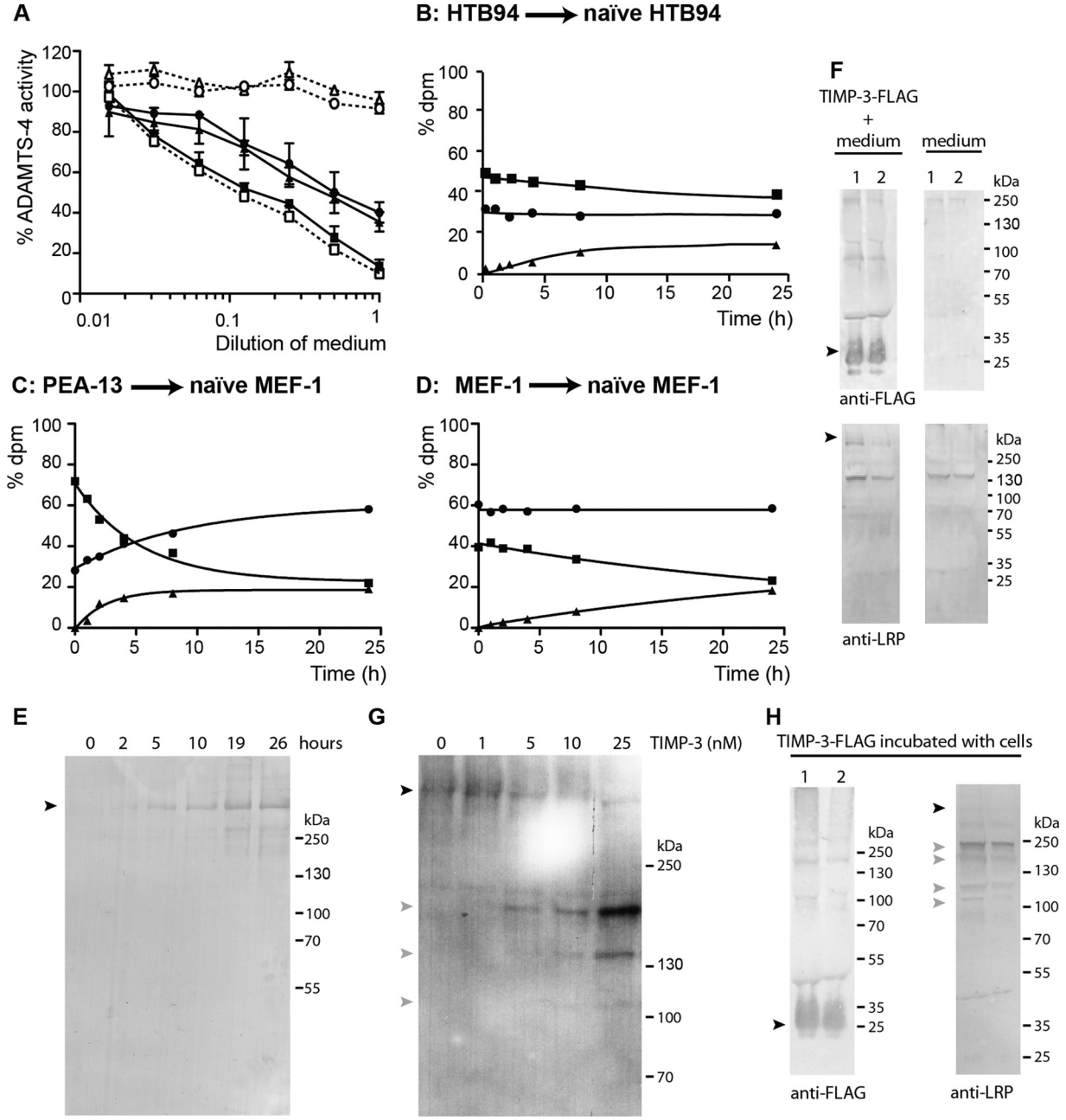

FIGURE 4. **sLRP-1 interacts with TIMP-3 and inhibits its endocytosis.** *A*, ADAMTS-4 (1 nM) was incubated (1 h, 37 °C) with dilutions of recombinant TIMP-3 in TNC buffer (from 1 nM, □) or with dilutions of TIMP-3 (1 nM) incubated on HTB94 cells for 0 h (■), 24 h (▲), or 48 h (●). As a control, ADAMTS-4 was incubated with conditioned medium from HTB94 cells incubated in serum-free medium without TIMP-3 for 24 h (○) or 48 h (△). Residual activity against FAM-AE∼L-QGRPISIAK-TAMRA was determined. *B*, [^{35}S]TIMP-3 (1 nM) was added to HTB94 cells for 24 h, after which conditioned media were harvested and transferred to naïve HTB94 cells for a further 0–24 h. Radioactivity in the cell-associated fraction (▲) as well as in the TCA-insoluble ■) and TCA-soluble (●) fractions of the conditioned media was quantified by counting radioactivity. This result is representative of three separate experiments. *C*, [^{35}S]TIMP-3 (1 nM) was added to PEA-13 cells for 24 h, after which conditioned media were harvested and transferred to fresh MEF-1 cells. Radioactivity in the cell-associated fraction (▲) as well as in the TCA-insoluble (■) and TCA-soluble (●) fractions of the conditioned media was quantified by scintillation counting (representative of two separate experiments). *D*, [^{35}S]TIMP-3 (1 nM) was added to MEF-1 cells for 24 h, after which conditioned media were harvested and transferred to naïve MEF-1 cells. Radioactivity in the cell-associated fraction (▲) as well as in the TCA-insoluble (■) and TCA-soluble (●) fractions of the conditioned media was quantified by scintillation counting. This result is representative of two separate experiments. *E*, conditioned medium harvested from HTB94 cells at different times was analyzed by SDS-PAGE and immunoblotting using 8G1 anti-LRP-1 antibody. *F*, conditioned medium collected from HTB94 cells was incubated with or without TIMP-3-FLAG (1 nM, overnight, room temperature) applied to an M2 anti-FLAG resin. The resin was washed extensively with TBS and then with 1 M NaCl in TBS to remove unspecific binding. Subsequently the resin was sequentially eluted with 200 μg/ml FLAG peptide in TBS (2 × 0.5 ml, *lanes 1* and *2*). Eluted samples were analyzed by SDS-PAGE and immunoblotting using M2 anti-FLAG and 8G1 anti-LRP-1 antibodies. *G*, different concentrations of TIMP-3 (0–25 nM) were incubated with HTB94 cells (24 h, 37 °C). Conditioned media were harvested and analyzed by SDS-PAGE and immunoblotting using 8G1 anti-LRP-1 antibody. *H*, TIMP-3-FLAG was incubated with HTB94 cells (1 nM, 24 h, 37 °C). The conditioned medium containing TIMP-3-FLAG remnants was harvested and applied to an M2 anti-FLAG resin. The resin was washed extensively with TBS and then with 1 M NaCl in TBS to remove unspecific binding. Subsequently the resin was sequentially eluted with 200 μg/ml FLAG peptide in TBS (2 × 0.5 ml, *lanes 1* and *2*). Eluted samples were analyzed by SDS-PAGE and immunoblotting using M2 anti-FLAG and 8G1 anti-LRP-1 antibodies.

LRP-1 and generation of LRP-1 fragments. A previous report showed that N-TIMP-3 inhibited MT1-MMP- and ADAM12-mediated shedding of LRP-1 (36). We found that, unlike TIMP-3, N-TIMP-3 did not induce shedding and fragmentation of LRP-1[4]; therefore, we hypothesize that the C-terminal domain of TIMP-3 can play a crucial role in this process. GM6001 has also been shown to inhibit LRP-1 shedding from macrophages and lung fibroblasts (21, 35), but we found that GM6001 had no effect on the rate of [^{35}S]TIMP-3 endocytosis by HTB94 cells. This suggests that a GM6001-insensitive sheddase may mediate LRP-1 shedding in HTB94 cells. The stimulus and sheddases responsible for LRP-1 constitutive shedding and TIMP-3-induced shedding in HTB94 cells and chondrocytes are currently under investigation in our laboratory.

Shedding of LRP-1 has numerous consequences. First, it can reduce endocytosis of LRP-1 ligands in a loss-of-function manner by reducing the number of endocytic receptors on the cell surface (21, 36, 38). Second, sLRP-1 can bind to and inhibit endocytosis of its ligands, as we found for TIMP-3, and as has been reported for tissue-type plasminogen activator (32). By antagonizing LRP-1-mediated endocytosis, sLRP-1 can increase the half-life of TIMP-3 in the extracellular space. More importantly, we found that the TIMP-3-sLRP-1 complex is still able to inhibit metalloproteinases. We found that the ratio between cell surface LRP-1 and sLRP-1 is an important factor that regulates the bioavailability of TIMP-3 in the extracellular space and hence controls ECM proteolysis and proteolysis of cell surface molecules.

In addition to the LRP-1-mediated pathway, we observed LRP-1-independent endocytosis of TIMP-3 in PEA-13 cells and RAP-treated HTB94, MEFs, and CHO cells. Although this is a slower process compared with the LRP-1-mediated endocytosis, it is likely to be receptor-mediated. Members belonging to the macrophage mannose receptor protein family may be possible candidates because they have been shown to internalize some LRP-1 ligands and play a crucial role in ECM turnover. For instance, urokinase plasminogen activator receptor-associated protein/endocytic recycling protein Endo180 is expressed in chondrocytes and fibroblasts and is involved in collagen internalization (40, 41). TIMP-1 and TIMP-2 are also endocytosed by LRP-1 (42, 43). Whereas TIMP-1 is internalized only in complex with MMP-9, with the binding determinants thought to reside on the MMP-9 (42). TIMP-2 can be endocytosed by LRP-1 both as a free inhibitor and in complex with MMP-2 or proMMP-2 (43). Interestingly, binding of TIMP-2 to HT1080 cells was insensitive to RAP, suggesting that TIMP-2 initially binds to a cell surface receptor other than LRP-1 prior to endocytosis (43). Furthermore, endocytosis and degradation of TIMP-2 were only partially inhibited by RAP, indicating that an LRP-1-independent endocytic pathway also occurs (43). These studies thus suggest that both TIMP-2 and TIMP-3 can be endocytosed by LRP-1-dependent and LRP-1-independent pathways. It would be interesting to determine whether TIMP-2 and TIMP-3 share the same mechanism of LRP-1-independent endocytosis.

Endocytosis of TIMP-3 in all tested cell types was almost completely inhibited by heparin. This suggested that an HSPG or CSPG might participate in TIMP-3 endocytosis, either as a direct endocytic receptor or as a co-receptor of LRP-1. HSPGs have been demonstrated to mediate endocytosis of ligands including lipoproteins (44). Alternatively, HSPGs might act as co-receptors of LRP-1-mediated endocytosis as proposed for thrombospondin 1 (45), tissue factor pathway inhibitor (46), amyloid-β (47), and factor VIII (48). However, we found that TIMP-3 endocytosis was not affected in xylosyltransferase-deficient CHO-745 cells, indicating that sulfated cell surface proteoglycans are not required for TIMP-3 endocytosis. In line with this finding, TIMP-3 endocytosis was also unimpaired in syndecan-4-null and syndecan-1-silenced cells. We therefore conclude that cell surface HSPG or CSPG does not mediate the LRP-1-independent pathway of TIMP-3 endocytosis.

The unimpaired endocytosis of TIMP-3 in CHO-745 cells nullified our hypothesis that heparin inhibits TIMP-3 endocytosis by blocking interaction with a sulfated cell surface proteoglycan component of the endocytic pathway. Interestingly, heparin has been shown to directly inhibit interaction of other ligands, including factor IXa (49), apolipoprotein A-V (50), C4b-binding protein (51) and PAI-1 (52), to LRP-1. In the case of PAI-1, the heparin binding and LRP-1 binding regions have been found to overlap (53, 54). Binding of proteins to heparin is commonly mediated by clusters of positively charged residues (55). Similarly, binding of protein ligands to LRP-1 and related LDL receptors is often mediated by positive residues, as has been demonstrated for RAP (56, 57) and α_2-microglobulin (58). In the case of RAP, crystallography and mutagenesis studies have confirmed that K256 and K270 mediate binding to acidic pockets in the ligand binding motifs of the receptor (56, 57). Inhibition of TIMP-3 binding to sLRP-1 by heparin suggests that the heparin binding and LRP-1 binding sites of TIMP-3 may also overlap. The three-dimensional structure of full-length TIMP-3 is currently unavailable, but the protein is predicted to contain an extended patch of basic residues, located on the opposite face of the protein to the inhibitory ridge that interacts with metalloproteinase. This may explain why TIMP-3-sLRP-1 complexes retain metalloproteinases inhibition activity.

The phenotypes of the *Timp3*$^{-/-}$ mouse reveal the central role of TIMP-3 in regulating activity of MMPs, ADAMs, and ADAMTSs. Our study has shown that LRP-1 plays an important role in controlling the extracellular levels of TIMP-3. It is well established that TIMP-3 binds to ECM (2, 3), but we have shown here that secreted TIMP-3 can be readily internalized via LRP-1, and this process competes with TIMP-3 binding to the ECM. On the other hand, shed sLRP-1 sequesters TIMP-3 from the above two reactions and increases its availability to extracellular MMPs, ADAMs and ADAMTs. It is notable that shedding of LRP-1 is increased under inflammatory conditions. We therefore propose that LPR-1 is a master regulator of extracellular trafficking of TIMP-3, and the ratio of cell surface LPR-1 and sLRP-1 dictates TIMP-3 availability.

Acknowledgments—We thank Prof. John Couchman of Copenhagen University for the syndecan-4-deficient cells, Prof. Akira Ito of Tokyo University for human uterine cervical fibroblasts, and Prof. Jeffrey Esko of University of California San Diego for CHO-K1 and CHO-745 cells.

REFERENCES

1. Brew, K., and Nagase, H. (2010) The tissue inhibitors of metalloproteinases (TIMPs): an ancient family with structural and functional diversity. *Biochim. Biophys. Acta* **1803,** 55–71
2. Staskus, P. W., Masiarz, F. R., Pallanck, L. J., and Hawkes, S. P. (1991) The 21-kDa protein is a transformation-sensitive metalloproteinase inhibitor of chicken fibroblasts. *J. Biol. Chem.* **266,** 449–454
3. Yu, W. H., Yu, S., Meng, Q., Brew, K., and Woessner, J. F. (2000) TIMP-3 binds to sulfated glycosaminoglycans of the extracellular matrix. *J. Biol. Chem.* **275,** 31226–31232
4. Leco, K. J., Waterhouse, P., Sanchez, O. H., Gowing, K. L., Poole, A. R., Wakeham, A., Mak, T. W., and Khokha, R. (2001) Spontaneous air space enlargement in the lungs of mice lacking tissue inhibitor of metalloproteinases-3 (TIMP-3). *J. Clin. Invest.* **108,** 817–829
5. Fedak, P. W., Smookler, D. S., Kassiri, Z., Ohno, N., Leco, K. J., Verma, S., Mickle, D. A., Watson, K. L., Hojilla, C. V., Cruz, W., Weisel, R. D., Li, R. K., and Khokha, R. (2004) TIMP-3 deficiency leads to dilated cardiomyopathy. *Circulation* **110,** 2401–2409
6. Fata, J. E., Leco, K. J., Voura, E. B., Yu, H. Y., Waterhouse, P., Murphy, G., Moorehead, R. A., and Khokha, R. (2001) Accelerated apoptosis in the TIMP-3-deficient mammary gland. *J. Clin. Invest.* **108,** 831–841
7. Sahebjam, S., Khokha, R., and Mort, J. S. (2007) Increased collagen and aggrecan degradation with age in the joints of Timp3$^{-/-}$ mice. *Arthritis Rheum.* **56,** 905–909
8. Mohammed, F. F., Smookler, D. S., Taylor, S. E., Fingleton, B., Kassiri, Z., Sanchez, O. H., English, J. L., Matrisian, L. M., Au, B., Yeh, W. C., and Khokha, R. (2004) Abnormal TNF activity in Timp3$^{-/-}$ mice leads to chronic hepatic inflammation and failure of liver regeneration. *Nat. Genet.* **36,** 969–977
9. Martin, E. L., Moyer, B. Z., Pape, M. C., Starcher, B., Leco, K. J., and Veldhuizen, R. A. (2003) Negative impact of tissue inhibitor of metalloproteinase-3 null mutation on lung structure and function in response to sepsis. *Am. J. Physiol. Lung Cell Mol. Physiol.* **285,** L1222–1232
10. Cardellini, M., Menghini, R., Martelli, E., Casagrande, V., Marino, A., Rizza, S., Porzio, O., Mauriello, A., Solini, A., Ippoliti, A., Lauro, R., Folli, F., and Federici, M. (2009) TIMP3 is reduced in atherosclerotic plaques from subjects with type 2 diabetes and increased by SirT1. *Diabetes* **58,** 2396–2401
11. Su, S., DiBattista, J. A., Sun, Y., Li, W. Q., and Zafarullah, M. (1998) Up-regulation of tissue inhibitor of metalloproteinases-3 gene expression by TGF-β in articular chondrocytes is mediated by serine/threonine and tyrosine kinases. *J. Cell Biochem.* **70,** 517–527
12. Li, W. Q., and Zafarullah, M. (1998) Oncostatin M up-regulates tissue inhibitor of metalloproteinases-3 gene expression in articular chondrocytes via *de novo* transcription, protein synthesis, and tyrosine kinase- and mitogen-activated protein kinase-dependent mechanisms. *J. Immunol.* **161,** 5000–5007
13. Darnton, S. J., Hardie, L. J., Muc, R. S., Wild, C. P., and Casson, A. G. (2005) Tissue inhibitor of metalloproteinase-3 (TIMP-3) gene is methylated in the development of esophageal adenocarcinoma: loss of expression correlates with poor prognosis. *Int. J. Cancer* **115,** 351–358
14. Gabriely, G., Wurdinger, T., Kesari, S., Esau, C. C., Burchard, J., Linsley, P. S., and Krichevsky, A. M. (2008) MicroRNA 21 promotes glioma invasion by targeting matrix metalloproteinase regulators. *Mol. Cell. Biol.* **28,** 5369–5380
15. Garofalo, M., Di Leva, G., Romano, G., Nuovo, G., Suh, S. S., Ngankeu, A., Taccioli, C., Pichiorri, F., Alder, H., Secchiero, P., Gasparini, P., Gonelli, A., Costinean, S., Acunzo, M., Condorelli, G., and Croce, C. M. (2009) miR-221&222 regulate TRAIL resistance and enhance tumorigenicity through PTEN and TIMP3 downregulation. *Cancer Cell* **16,** 498–509
16. Wang, B., Hsu, S. H., Majumder, S., Kutay, H., Huang, W., Jacob, S. T., and Ghoshal, K. (2010) TGFβ-mediated upregulation of hepatic miR-181b promotes hepatocarcinogenesis by targeting TIMP3. *Oncogene* **29,** 1787–1797
17. Limana, F., Esposito, G., D'Arcangelo, D., Di Carlo, A., Romani, S., Melillo, G., Mangoni, A., Bertolami, C., Pompilio, G., Germani, A., and Capogrossi, M. C. (2011) HMGB1 attenuates cardiac remodelling in the failing heart via enhanced cardiac regeneration and miR-206-mediated inhibition of TIMP-3. *PLoS One* **6,** e19845
18. Troeberg, L., Fushimi, K., Khokha, R., Emonard, H., Ghosh, P., and Nagase, H. (2008) Calcium pentosan polysulfate is a multifaceted exosite inhibitor of aggrecanases. *FASEB J.* **22,** 3515–3524
19. Strickland, D. K., Gonias, S. L., and Argraves, W. S. (2002) Diverse roles for the LDL receptor family. *Trends Endocrinol. Metab.* **13,** 66–74
20. Lillis, A. P., Mikhailenko, I., and Strickland, D. K. (2005) Beyond endocytosis: LRP function in cell migration, proliferation and vascular permeability. *J. Thromb. Haemost.* **3,** 1884–1893
21. Wygrecka, M., Wilhelm, J., Jablonska, E., Zakrzewicz, D., Preissner, K. T., Seeger, W., Guenther, A., and Markart, P. (2011) Shedding of low density lipoprotein receptor–related protein-1 in acute respiratory distress syndrome. *Am. J. Respir. Crit Care Med.* **184,** 438–448
22. Selvais, C., Gaide Chevronnay, H. P., Lemoine, P., Dedieu, S., Henriet, P., Courtoy, P. J., Marbaix, E., and Emonard, H. (2009) Metalloproteinase-dependent shedding of low density lipoprotein receptor-related protein-1 ectodomain decreases endocytic clearance of endometrial matrix metalloproteinase-2 and -9 at menstruation. *Endocrinology* **150,** 3792–3799
23. Liu, Q., Zhang, J., Tran, H., Verbeek, M. M., Reiss, K., Estus, S., and Bu, G. (2009) LRP1 shedding in human brain: roles of ADAM10 and ADAM17. *Mol. Neurodegener.* **4,** 17
24. Chung, L., Shimokawa, K., Dinakarpandian, D., Grams, F., Fields, G. B., and Nagase, H. (2000) Identification of the ^{183}RWTNNFREY^{191} region as a critical segment of matrix metalloproteinase 1 for the expression of collagenolytic activity. *J. Biol. Chem.* **275,** 29610–29617
25. Nielsen, M. S., Nykjaer, A., Warshawsky, I., Schwartz, A. L., and Gliemann, J. (1995) Analysis of ligand binding to the α2-macroglobulin receptor/low density lipoprotein receptor-related protein: evidence that lipoprotein lipase and the carboxyl-terminal domain of the receptor-associated protein bind to the same site. *J. Biol. Chem.* **270,** 23713–23719
26. Kashiwagi, M., Enghild, J. J., Gendron, C., Hughes, C., Caterson, B., Itoh, Y., and Nagase, H. (2004) Altered proteolytic activities of ADAMTS-4 expressed by C-terminal processing. *J. Biol. Chem.* **279,** 10109–10119
27. Troeberg, L., Fushimi, K., Scilabra, S. D., Nakamura, H., Dive, V., Thøgersen, I. B., Enghild, J. J., and Nagase, H. (2009) The C-terminal domains of ADAMTS-4 and ADAMTS-5 promote association with N-TIMP-3. *Matrix Biol.* **28,** 463–469
28. Esko, J. D., Stewart, T. E., and Taylor, W. H. (1985) Animal cell mutants defective in glycosaminoglycan biosynthesis. *Proc. Natl. Acad. Sci. U.S.A.* **82,** 3197–3201
29. Willnow, T. E., and Herz, J. (1994) Genetic deficiency in low density lipoprotein receptor-related protein confers cellular resistance to *Pseudomonas* endotoxin A: evidence that this protein is required for uptake and degradation of multiple ligands *J. Cell Sci.* **107,** 719–726
30. Ishiguro, K., Kadomatsu, K., Kojima, T., Muramatsu, H., Tsuzuki, S., Nakamura, E., Kusugami, K., Saito, H., and Muramatsu, T. (2000) Syndecan-4 deficiency impairs focal adhesion formation only under restricted conditions. *J. Biol. Chem.* **275,** 5249–5252
31. Gendron, C., Kashiwagi, M., Hughes, C., Caterson, B., and Nagase, H. (2003) TIMP-3 inhibits aggrecanase-mediated glycosaminoglycan release from cartilage explants stimulated by catabolic factors. *FEBS Lett.* **555,** 431–436
32. Quinn, K. A., Grimsley, P. G., Dai, Y. P., Tapner, M., Chesterman, C. N., and Owensby, D. A. (1997) Soluble low density lipoprotein receptor-related protein (LRP) circulates in human plasma. *J. Biol. Chem.* **272,** 23946–23951
33. Echtermeyer, F., Baciu, P. C., Saoncella, S., Ge, Y., and Goetinck, P. F. (1999) Syndecan-4 core protein is sufficient for the assembly of focal adhesions and actin stress fibers. *J. Cell Sci.* **112,** 3433–3441
34. Ahonen, M., Poukkula, M., Baker, A. H., Kashiwagi, M., Nagase, H., Eriksson, J. E., and Kähäri, V. M. (2003) Tissue inhibitor of metalloproteinases-3 induces apoptosis in melanoma cells by stabilization of death receptors. *Oncogene* **22,** 2121–2134
35. Gorovoy, M., Gaultier, A., Campana, W. M., Firestein, G. S., and Gonias, S. L. (2010) Inflammatory mediators promote production of shed LRP1/CD91, which regulates cell signaling and cytokine expression by macrophages. *J. Leukocyte Biol.* **88,** 769–778

36. Selvais, C., D'Auria, L., Tyteca, D., Perrot, G., Lemoine, P., Troeberg, L., Dedieu, S., Noël, A., Nagase, H., Henriet, P., Courtoy, P. J., Marbaix, E., and Emonard, H. (2011) Cell cholesterol modulates metalloproteinase-dependent shedding of low density lipoprotein receptor-related protein-1 (LRP-1) and clearance function. *FASEB J.* **25,** 2770–2781
37. von Arnim, C. A., Kinoshita, A., Peltan, I. D., Tangredi, M. M., Herl, L., Lee, B. M., Spoelgen, R., Hshieh, T. T., Ranganathan, S., Battey, F. D., Liu, C. X., Bacskai, B. J., Sever, S., Irizarry, M. C., Strickland, D. K., and Hyman, B. T. (2005) The low density lipoprotein receptor-related protein (LRP) is a novel β-secretase (BACE1) substrate. *J. Biol. Chem.* **280,** 17777–17785
38. Rozanov, D. V., Hahn-Dantona, E., Strickland, D. K., and Strongin, A. Y. (2004) The low density lipoprotein receptor-related protein LRP is regulated by membrane type-1 matrix metalloproteinase (MT1-MMP) proteolysis in malignant cells. *J. Biol. Chem.* **279,** 4260–4268
39. Quinn, K. A., Pye, V. J., Dai, Y. P., Chesterman, C. N., and Owensby, D. A. (1999) Characterization of the soluble form of the low density lipoprotein receptor-related protein (LRP). *Exp. Cell Res.* **251,** 433–441
40. Engelholm, L. H., List, K., Netzel-Arnett, S., Cukierman, E., Mitola, D. J., Aaronson, H., Kjøller, L., Larsen, J. K., Yamada, K. M., Strickland, D. K., Holmbeck, K., Danø, K., Birkedal-Hansen, H., Behrendt, N., and Bugge, T. H. (2003) uPARAP/Endo180 is essential for cellular uptake of collagen and promotes fibroblast collagen adhesion. *J. Cell Biol.* **160,** 1009–1015
41. Kjøller, L., Engelholm, L. H., Høyer-Hansen, M., Danø, K., Bugge, T. H., and Behrendt, N. (2004) uPARAP/endo180 directs lysosomal delivery and degradation of collagen IV. *Exp. Cell Res.* **293,** 106–116
42. Hahn-Dantona, E., Ruiz, J. F., Bornstein, P., and Strickland, D. K. (2001) The low density lipoprotein receptor-related protein modulates levels of matrix metalloproteinase 9 (MMP-9) by mediating its cellular catabolism. *J. Biol. Chem.* **276,** 15498–15503
43. Emonard, H., Bellon, G., Troeberg, L., Berton, A., Robinet, A., Henriet, P., Marbaix, E., Kirkegaard, K., Patthy, L., Eeckhout, Y., Nagase, H., Hornebeck, W., and Courtoy, P. J. (2004) Low density lipoprotein receptor-related protein mediates endocytic clearance of pro-MMP-2·TIMP-2 complex through a thrombospondin-independent mechanism. *J. Biol. Chem.* **279,** 54944–54951
44. Stanford, K. I., Bishop, J. R., Foley, E. M., Gonzales, J. C., Niesman, I. R., Witztum, J. L., and Esko, J. D. (2009) Syndecan-1 is the primary heparan sulfate proteoglycan mediating hepatic clearance of triglyceride-rich lipoproteins in mice. *J. Clin. Invest.* **119,** 3236–3245
45. Wang, S., Herndon, M. E., Ranganathan, S., Godyna, S., Lawler, J., Argraves, W. S., and Liau, G. (2004) Internalization but not binding of thrombospondin-1 to low density lipoprotein receptor-related protein-1 requires heparan sulfate proteoglycans. *J. Cell. Biochem.* **91,** 766–776
46. Schwartz, A. L., and Broze, G. J., Jr. (1997) Tissue factor pathway inhibitor endocytosis. *Trends Cardiovasc. Med.* **7,** 234–239
47. Kanekiyo, T., Zhang, J., Liu, Q., Liu, C. C., Zhang, L., and Bu, G. (2011) Heparan sulphate proteoglycan and the low density lipoprotein receptor-related protein 1 constitute major pathways for neuronal amyloid-β uptake. *J. Neurosci.* **31,** 1644–1651
48. Sarafanov, A. G., Ananyeva, N. M., Shima, M., and Saenko, E. L. (2001) Cell surface heparan sulfate proteoglycans participate in factor VIII catabolism mediated by low density lipoprotein receptor-related protein. *J. Biol. Chem.* **276,** 11970–11979
49. Neels, J. G., van Den Berg, B. M., Mertens, K., ter Maat, H., Pannekoek, H., van Zonneveld, A. J., and Lenting, P. J. (2000) Activation of factor IX zymogen results in exposure of a binding site for low density lipoprotein receptor-related protein. *Blood* **96,** 3459–3465
50. Nilsson, S. K., Lookene, A., Beckstead, J. A., Gliemann, J., Ryan, R. O., and Olivecrona, G. (2007) Apolipoprotein A-V interaction with members of the low density lipoprotein receptor gene family. *Biochemistry* **46,** 3896–3904
51. Westein, E., Denis, C. V., Bouma, B. N., and Lenting, P. J. (2002) The α-chains of C4b-binding protein mediate complex formation with low density lipoprotein receptor-related protein. *J. Biol. Chem.* **277,** 2511–2516
52. Nykjaer, A., Petersen, C. M., Møller, B., Jensen, P. H., Moestrup, S. K., Holtet, T. L., Etzerodt, M., Thøgersen, H. C., Munch, M., and Andreasen, P. A. (1992) Purified α2-macroglobulin receptor/LDL receptor-related protein binds urokinase-plasminogen activator inhibitor type-1 complex: evidence that the α2-macroglobulin receptor mediates cellular degradation of urokinase receptor-bound complexes. *J. Biol. Chem.* **267,** 14543–14546
53. Horn, I. R., van den berg, B. M., Moestrup, S. K., Pannekoek, H., and van Zonneveld, A. J. (1998) Plasminogen activator inhibitor 1 contains a cryptic high affinity receptor binding site that is exposed upon complex formation with tissue-type plasminogen activator. *Thromb. Haemost.* **80,** 822–828
54. Stefansson, S., Muhammad, S., Cheng, X. F., Battey, F. D., Strickland, D. K., and Lawrence, D. A. (1998) Plasminogen activator inhibitor-1 contains a cryptic high affinity binding site for the low density lipoprotein receptor-related protein. *J. Biol. Chem.* **273,** 6358–6366
55. Gandhi, N. S., and Mancera, R. L. (2008) The structure of glycosaminoglycans and their interactions with proteins. *Chem. Biol. Drug Des.* **72,** 455–482
56. Fisher, C., Beglova, N., and Blacklow, S. C. (2006) Structure of an LDLR-RAP complex reveals a general mode for ligand recognition by lipoprotein receptors. *Mol. Cell* **22,** 277–283
57. van den Biggelaar, M., Sellink, E., Klein Gebbinck, J. W., Mertens, K., and Meijer, A. B. (2011) A single lysine of the two-lysine recognition motif of the D3 domain of receptor-associated protein is sufficient to mediate endocytosis by low density lipoprotein receptor-related protein. *Int. J. Biochem. Cell Biol.* **43,** 431–440
58. Arandjelovic, S., Hall, B. D., and Gonias, S. L. (2005) Mutation of lysine 1370 in full-length human α2-macroglobulin blocks binding to the low density lipoprotein receptor-related protein-1. *Arch Biochem. Biophys.* **438,** 29–35